Small Molecule Nitazoxanide Inhibits Osteogenic Differentiation and Promotes Adipogenic Differentiation of Bone Marrow Mesenchymal Stem Cells

Chan Yuan JIN[1#], Yan Yan GUO[1#], Xiao Mei HOU[1], Zhi Hui TANG[1]

Objective: *To investigate the potential effect of small molecule nitazoxanide (NTZ) on the osteogenic and adipogenic differentiation of bone marrow mesenchymal stem cells (BMSCs).*
Methods: *Cell counting Kit-8 assay was used to examine the effect of NTZ on proliferation of BMSCs. Quantitative reverse transcription polymerase chain reaction (qRT-PCR) and Western blot analysis were used to measure the expression of osteogenic and adipogenic marker gene. Alkaline phosphatase (ALP) staining and activity assay and Alizarin Red S (ARS) staining were used to investigate the effect of NTZ on osteogenesis. Oil red O (ORO) staining assay was used to assess the impact of NTZ on adipogenesis.*
Results: *NTZ significantly suppressed the osteogenic differentiation but promoted the adipogenic differentiation of BMSCs. Mechanistically, NTZ regulated osteogenic/adipogenic differentiation of BMSCs by inhibiting the Wnt/β-catenin signalling pathway. The addition of Wnt/β-catenin signalling pathway activator, lithium chloride, could reverse the effect of NTZ on BMSCs.*
Conclusion: *NTZ affected osteogenic and adipogenic differentiation of BMSCs with the involvement of Wnt/β-catenin signalling pathway. This finding expanded the understanding of NTZ pharmacology and indicated that NTZ might have an adverse effect on bone homeostasis.*
Key words: *adipogenesis, bone marrow mesenchymal stem cells, nitazoxanide, osteogenesis, Wnt/β-catenin pathway*
Chin J Dent Res 2023;26(2):69–75; doi: 10.3290/j.cjdr.b4128019

In recent years, monoclonal antibodies, small molecule drugs and nanozymes have attracted widespread attention from scientific researchers and clinicians due to their broad application prospects in targeted therapies[1-8]. Small molecule nitazoxanide or 2-(acetyloxy)-N-(5-nitro-2-thiazolyl) benzamide, usually shortened to NTZ, was first successfully synthesized in the 1970s and initially used as an antiparasitic drug for intestinal protozoa and helminths[9-11]. Since the late 1990s, NTZ has been found to have antiviral activity against a brand range of both RNA and DNA viruses, including coronaviruses, hepatitis B virus (HBV), influenza and other viruses[12-14]. Recently, NTZ was found to exhibit efficient antiviral activity against severe acute respiratory syndrome coronavirus 2 (SARS-CoV-2), a pandemic RNA virus belonging to the genera of betacoronaviridae. Many studies have demonstrated that NTZ, an FDA approved, safe and inexpensive old drug, has great application potential for repurposing against coronavirus disease 2019 (COVID-19)[15-17]. Many small molecule drugs have been found to have an effect on differentiation of bone marrow mesenchymal stem cells (BMSCs)[18]. Our research group previously found the small molecule anti-inflammatory drug sulfasalazine could promote osteogenic differentiation of BMSCs[19]; however, it is unclear whether NTZ affects osteogenic and adipogenic differentiation of BMSCs.

BMSCs are multipotent cells that have the potential to differentiate into various kinds of cell types, for example osteoblasts, adipocytes, chondrocytes and myoblasts[20-23]. Normally, there is a reciprocal balance between adipogenesis and osteogenesis, which is some-

1 Second Dental Center, Peking University School and Hospital of Stomatology, National Center for Stomatology, National Clinical Research Center for Oral Diseases, Beijing, P.R. China.
# These two authors contributed equally to this work.

Corresponding authors: Dr Xiao Mei HOU and Dr Zhi Hui TANG, The Second Clinical Division of Peking University School and Hospital of Stomatology, B5 Anli Garden, #66 Anli Road, Chao Yang District, Beijing 100101, P.R. China. Tel: 86-10-82196299; Fax: 86-10-64907970. Email: houxiaoMei1108@163.com; tang_zhihui@live.cn

times disrupted in various human disorders including osteoporosis and obesity[24-28]. Numerous studies have shown that complex signalling pathways, including the Wnt/β-catenin and Hedgehog signalling pathways, were involved in regulating the osteogenic and adipogenic differentiation of BMSCs[29-33]. The Wnt/β-catenin signalling pathway has been found to promote osteogenic differentiation of BMSCs and plays a crucial role in bone homeostasis. It is activated when the Wnt ligands bind to the cell surface receptors and induces the accumulation of β-catenin in the cytoplasm and its final translocation into the nucleus. Consequently, β-catenin interacts with T-cell factor/lymphoid enhancing factor (TCF/LEF) to upregulate the expression of various target genes[34,35].

In the present study, we investigated the effects of NTZ on the osteogenic/adipogenic differentiation of BMSCs in vitro and suggested the potential effect of NTZ on bone health.

Materials and methods

Cell culture and reagent treatment

BMSCs were obtained from ScienCell Research Laboratories (Carlsbad, CA, USA). The proliferation medium (PM) consisted of Dulbecco's Modified Eagle Medium (DMEM), supplemented with 10% foetal bovine serum and 1% penicillin/streptomycin (all from Gibco, Grand Island, NY, USA), in a humidified incubator with an atmosphere containing 5% CO_2 at 37°C. The osteogenic medium (OM) was composed of PM supplemented with 100 nM dexamethasone, 0.2 mM ascorbic acid and 10 mM β-glycerophosphate (all from Sigma, St Louis, MO, USA). Similarly, adipogenic medium (AM) was composed of standard PM supplemented with 50 nm insulin,100 nM dexamethasone, 0.5mM 3-isobutyl-1-methylxanthine and 200 mM indomethacin (all from Sigma). Lithium chloride (LiCl) (5 mmol/L) was used to activate Wnt/β-catenin signalling[36]. The medium was refreshed every 2 days. All cell-based experiments were performed more than three times.

Cell counting kit-8 (CCK8) assay

Once 80% confluence had been achieved, BMSCs were seeded in 96-well plates, then the plates were incubated in an incubator with standard culture conditions (37°C, 5% CO_2 and 95% humidity) for 24 hours. Afterwards, they were treated with NTZ (0, 1, 10, 20 or 50 μM) in the presence of PM for 48 hours. The medium was replaced with fresh DMEM supplemented with 10% CCK8 solution (Bioscience, Shanghai, China), then the absorbance values at a wavelength of 450 nm were detected with the microplate reader (Bio-Rad, Hercules, CA, USA). 10 μM of NTZ was used in the following experiment.

RNA extraction and quantitative reverse transcription polymerase chain reaction (qRT-PCR) analysis

Total RNA was isolated from cells using TRIZOL reagent (Invitrogen, Carlsbad, CA, USA), and complementary DNA (cDNA) was synthesised using PrimeScript RT (Reagent Kit Takara, Tokyo, Japan). qRT-PCR was carried out in a 7500 Real-Time PCR assay system (Applied Biosystems, Foster City, CA, USA) with SYBR Green Master Mix (Roche Applied Science, Mannheim, Germany). The thermal cycling conditions were 95°C for 10 minutes, followed by 40 cycles of 95°C for 15 seconds and 60°C for 1 minute. Glyceraldehyde-3-phosphate dehydrogenase (GAPDH) was used as the internal control for the relative mRNA expression levels of target genes. The data was analysed using the $2^{-\Delta\Delta Ct}$ method. The primer sequences used were as follows: GAPDH, (F) GGTCACCAGGGCTGCTTTTA, (R) GGATCTCGCTCCTGGAAGATG; ALP, (F) ATGGGATGGGTGTCTCCACA, (R) CCACGAAGGGGAACTTGTC; RUNX2, (F) CCGCCTCAGTGATTTAGGGC, (R) GGGTCTGTAATCTGACTCTGTCC; PPARγ, (F) GAGGAGCCTAAGGTAAGGAG, (R) GTCATTTCGTTAAAGGCTGA.

Alkaline phosphatase (ALP) staining and activity

After a 7-day culture in PM or OM, the medium was removed. Cells were washed with 1× PBS and fixed with 4% paraformaldehyde for 10 minutes at room temperature, followed by incubation with a 5-bromo-4-chloro-3-indolylphosphate/nitro-blue-tetrazolium (BCIP/NBT) staining kit (CWBIO, Beijing, China) solution according to the instructions. The stained cells were observed under an inverted fluorescence microscope (Olympus, Tokyo, Japan).

ALP activity assay was conducted using the ALP Activity Kit (Biovision, Milpitas, CA, USA). The total protein of cells was determined with the BCA method using a Pierce protein assay kit (Thermo Fisher Scientific, Waltham, MA, USA). Finally, the absorbance values at 520 nm were determined using a spectrophotometry reader and normalised to the total protein content.

ARS staining and quantification

After a 14-day culture in PM or OM, cells were washed with 1× PBS, fixed with 4% paraformaldehyde for 10

minutes and rinsed with distilled water. After that, cells were stained with 1% ARS solution (Sigma) for 20 minutes at room temperature and images were acquired using a scanner. For ARS quantification, the cells were destained with cetyl-pyridinium chloride (Sigma), then absorbance was measured with a spectrophotometer at 570 nm.

ORO staining and quantification

After a 14-day culture in PM or AM, cells were washed three times with 1× PBS, fixed for 10 minutes in 4% paraformaldehyde and rinsed with 60% isopropyl alcohol. ORO (Sigma) staining solution was then added to each well for 10 minutes at room temperature. The lipid droplets of cells were observed and imaged under a microscope. For quantitative assessment, they were eluted with 100% isopropyl alcohol and measured with a spectrophotometer at 520 nm.

Western blot analysis

Cells were harvested, lysed and extracted in the ice-cold radio immunoprecipitation assay (RIPA) lysis buffer (HuaxingBio Science, Beijing, China) with 1:100 volume of PMSF (Sigma). The Pierce BCA protein assay kit was then used to measure the concentrations of the protein samples. Next, equal amounts of total protein from each sample were separated on a 10% sodium dodecyl sulfate polyacrylamide gel electrophoresis (SDD-PAGE) and transferred onto polyvinylidene fluoride (PVDF) membranes (Millipore, Billerica, MA, USA), then the membranes were blocked with fat-free milk in TBST for 60 minutes at room temperature and incubated overnight at 4˚C with primary antibodies against β-catenin (1:2000) (Cell Signaling Technology, Beverly, MA, USA), and GAPDH (1:5000) (HuaxingBio Science). After washing three times with TBST, the membranes were incubated with secondary antibodies (HuaxingBio Science) for 60 minutes at room temperature. The immunoreactive bands were detected using the ECL Western Blot Kit (CoWin Biotech, Beijing, China) and the intensity was quantified with ImageJ analysis software (National Institutes of Health, Bethesda, MD, USA).

Statistical analysis

All statistical analyses were performed using SPSS version 23.0 (SPSS, Chicago, IL, USA). Comparisons between two groups were analysed with independent two-tailed Student *t* tests, and comparisons among three or more groups were analysed using a one-way analysis of variance. Data were expressed as mean ± standard deviation (SD). $P < 0.05$ was considered statistically significant. All experiments were conducted independently at least three times.

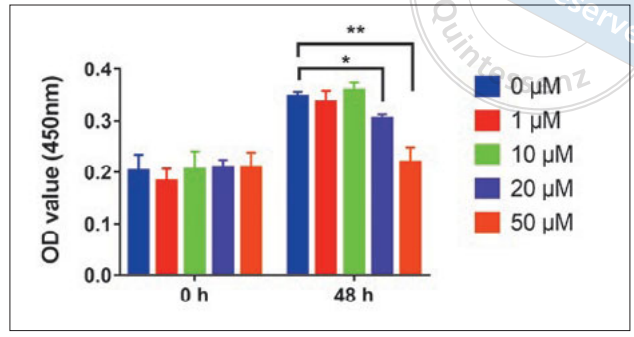

Fig 1 The effect of NTZ on the proliferation of BMSCs. The cell proliferation curve was observed by CCK8 assay. BMSCs were treated with various concentrations (0, 1, 10, 20 and 50 μM) of NTZ for 48 hours. The results were presented as mean ± SD (*$P < 0.05$, **$P < 0.01$ compared with 0 μM).

Results

The effect of NTZ on cell proliferation of BMSCs

First, we investigated whether NTZ could affect the proliferation of BMSCs using CCK8 assay. BMSCs were treated with different concentrations of NTZ (0, 1, 10, 20 and 50 μM) for 48 hours. As shown in Fig 1, NTZ at 20 and 50 μM could cause a significant reduction in the proliferation of BMSCs.

NTZ inhibited osteogenic differentiation of BMSCs

To elucidate whether NTZ has an impact on osteogenic differentiation of BMSCs, we added NTZ into the PM and OM. qRT-PCR showed that the mRNA expression levels of osteogenic marker genes RUNX family transcription factor 2 (RUNX2) and alkaline phosphatase (ALP) were markedly decreased after NTZ treatment (Figs 2a and b). In line with this, ALP and ARS staining demonstrated that NTZ reduced the mineral deposition significantly and inhibited the ALP activity of BMSCs (Figs 2c to f). All these data implied that NTZ suppressed the osteogenic differentiation of BMSCs.

NTZ promoted adipogenic differentiation of BMSCs

In general, osteogenic and adipogenic differentiation are two reverse directions of differentiation in BMSCs. Next, we assessed the role of NTZ in adipogenic differen-

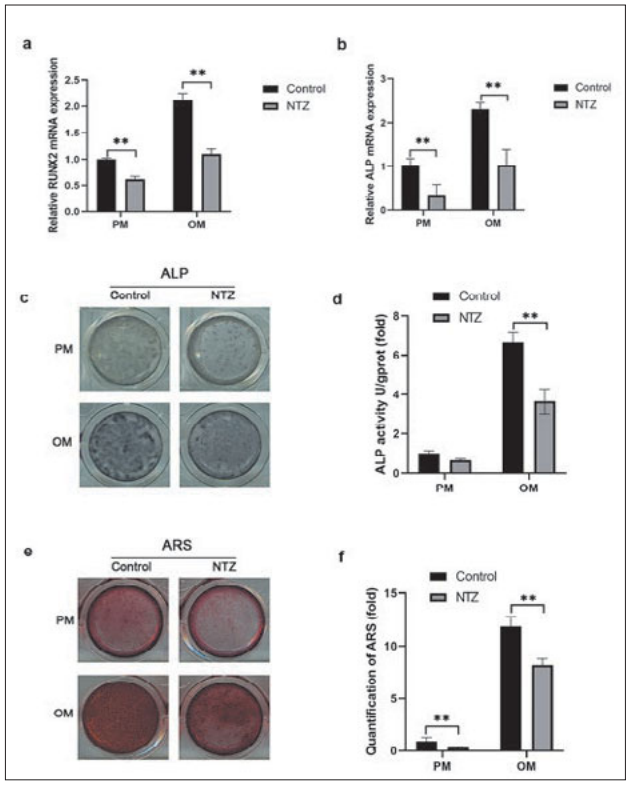

Fig 2 NTZ suppressed osteogenic differentiation of BMSCs. Cells were treated with proliferation medium (PM) or osteogenic medium (OM) and NTZ (10 μM) or DMSO (control) was added to the medium. **(a and b)** Relative mRNA expression levels of osteogenic markers (RUNX2 and ALP) were detected by qRT-PCR at day 5. **(c and d)** Representative images of ALP staining and quantification at day 7. **(e and f)** Representative images of ARS staining and quantification at day 14. The results were presented as mean ± SD (***P* < 0.01 compared with control).

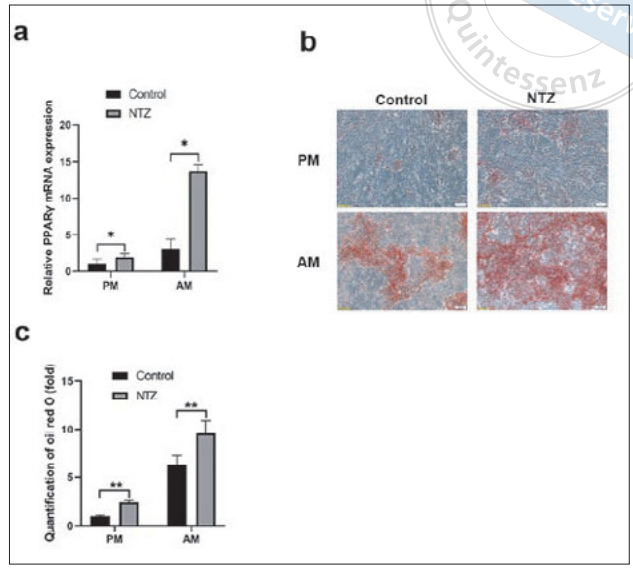

Fig 3 NTZ promoted adipogenic differentiation of BMSCs. Cells were treated with PM or adipogenic medium (AM) and NTZ (10 μM) or DMSO (control) was added to the medium. **(a)** Relative mRNA expression level of PPARγ was detected by qRT-PCR at day 5. **(b and c)** Representative images and quantification analysis of ORO staining at day 14. The results were presented as mean ± SD (**P* < 0.05, ***P* < 0.01 compared with control).

tiation of BMSCs. As expected, qRT-PCR results showed that the mRNA level of adipogenic marker gene peroxisome proliferator activated receptor γ (PPARγ) was markedly upregulated in the presence of NTZ (Fig 3a). In line with this result, ORO staining showed the lipid droplets were increased in the NTZ treated group (Figs 3b and c). Taken together, the results of qRT-PCR and ORO staining all suggested that NTZ has a positive effect on the adipogenic differentiation of BMSCs.

NTZ regulated differentiation of BMSCs via the Wnt/β-catenin pathway

Previous studies revealed that NTZ inhibited the Wnt/β-catenin signalling pathway in colorectal cancer cells. Thus, we hypothesised that NTZ regulated differentiation of BMSCs with the involvement of the Wnt/β-catenin signalling pathway. To confirm the mechanism, we first performed western blot analysis to detect the level of β-catenin after NTZ treatment. As shown in Figs 4a and b, the protein level of β-catenin was evidently downregulated in the NTZ group compared with the control group. Since LiCl is a well-established inhibitor of glycogen synthase kinase-3 and widely used as an agonist to activate Wnt/β-catenin signalling, we treated the NTZ group with LiCl to recover the level of β-catenin. qRT-PCR analyses showed that the effect of NTZ on the expression of RUNX2, ALP and PPARγ was significantly restored by LiCl treatment (Figs 4c to e). Collectively, these results revealed that NTZ suppressed the osteogenic differentiation of BMSCs and promoted the adipogenic differentiation via the Wnt/β-catenin signalling pathway.

Discussion

Small molecule NTZ, a thiazolide antiparasitic agent, has been widely commercialised for treating parasitic infection. In recent years, researchers have identified the antiviral activity and antitumoural effect of NTZ. To date, NTZ has been reported to have some common adverse effects, such as diarrhoea, abdominal pain,

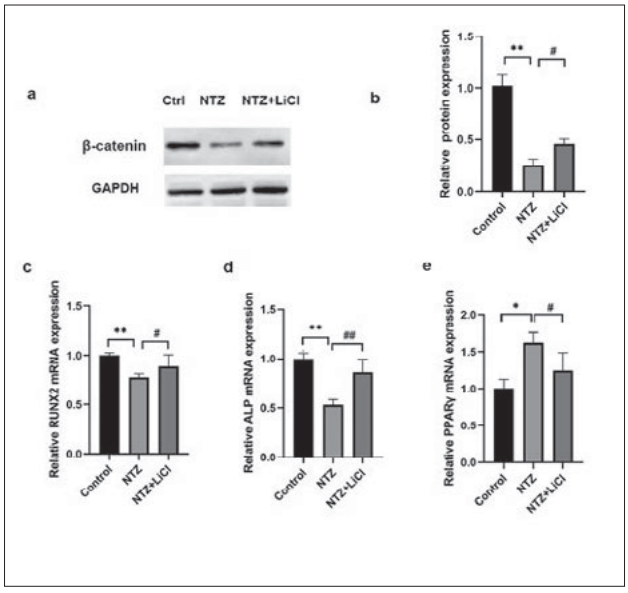

Fig 4 NTZ regulated differentiation of BMSCs by targeting the Wnt/β-catenin pathway. **(a)** Immunoblot images showing the protein expression of β-catenin after NTZ (10 μM) treatment or lithium chloride (LiCl) (5 mmol/L) treatment for 48 hours. DMSO was used as control group. Glyceraldehyde-3-phosphate dehydrogenase (GAPDH) was used as an internal control. **(b)** Quantification of **(a). (c-e)** Relative mRNA expression levels of RUNX2, ALP and PPARγ were examined by qRT-PCR at day 5. The results were presented as mean ± SD (*/#P < 0.05, **/##P < 0.01, *compared with control, # compared with NTZ group).

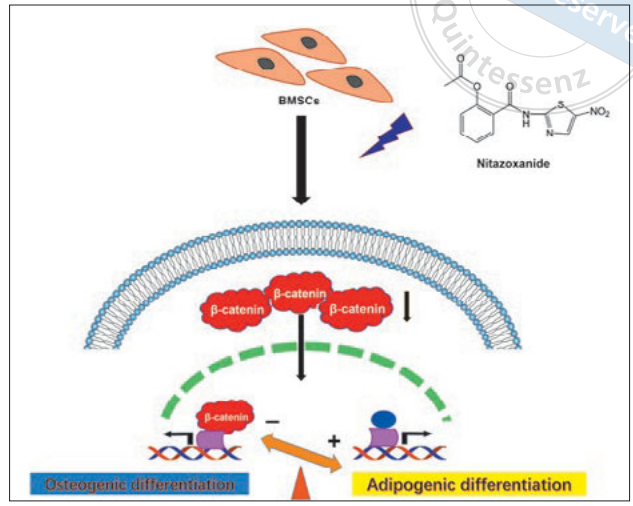

Fig 5 Schematic diagram of the effect of NTZ on osteogenic and adipogenic differentiation of BMSCs

headache and nausea[37-42]; however, its effect on BMSCs has not yet been reported.

Small molecule drugs refer to those drugs with a molecular weight ≤ 1000 Da. Recently, several small molecule drugs have been demonstrated to regulate osteogenic differentiation of BMSCs. For example, many studies have proved that the widely used cholesterol-lowering drug simvastatin promotes bone repair by upregulating BMP2 expression and activating osteogenesis-related pathways[43]. The conventional anticonvulsant drug valproic acid has recently been found to promote osteogenic differentiation of mesenchymal stem cells by inhibiting histone deacetylase[44]. The most commonly used antidiabetic drug metformin has also been discovered to promote osteogenic differentiation of rat bone marrow mesenchymal stem cells[45]. We wondered whether NTZ had an impact on osteogenic differentiation of BMSCs and performed a series of experiments. The results showed that NTZ negatively regulated osteogenic differentiation and upregulated adipogenic differentiation of BMSCs.

In this study, we found that NTZ regulated osteogenic and adipogenic differentiation through the Wnt/β-catenin signalling pathway; however, NTZ has been demonstrated to be able to regulate multiple signalling pathways. For example, Lü et al[46] found that NTZ inhibited the STAT3 pathway, Ye et al[47] found NTZ suppressed the AKT/mTOR pathway in osteosarcoma cells and Khan and Lee[48] revealed that NTZ might exert anti-hepatocellular carcinoma effects by affecting multiple signalling pathways, such as the MAPK signalling pathway. Thus, NTZ might regulate osteogenic and adipogenic differentiation via other signalling pathways. Besides, the effect of NTZ in vivo remains unclear. Further studies including animal experiments are required to clarify the effect and detailed mechanism of NTZ.

Conclusion

In summary (as shown in Fig 5), we investigated the function of small molecular NTZ in BMSCs and found that NTZ inhibited the osteogenic differentiation and promoted the adipogenic differentiation of BMSCs by inhibiting the Wnt/β-catenin pathway, suggesting that NTZ could pose a potential risk for bone health.

Conflicts of interest

The authors declare no conflicts of interest related to this study.

Author contribution

Dr Chan Yuan JIN designed the research, performed the experiments, collected and analysed the data, and drafted and revised the manuscript; Dr Yan Yan GUO per-

formed the experiments, collected the data and drafted the manuscript; Drs Xiao Mei HOU and Zhi Hui TANG supervised the work.

(Received Oct 13, 2022; accepted Mar 06, 2023)

References

1. Castelli MS, McGonigle P, Hornby PJ. The pharmacology and therapeutic applications of monoclonal antibodies. Pharmacol Res Perspect 2019;7:e00535.
2. Zhuang ZC, Li YH, Yu RH, et al. Reversely trapping atoms from a perovskite surface for high-performance and durable fuel cell cathodes. Nat Catal 2022;5:300–310.
3. Shi J, Shu R, Shi X, et al. Multi-activity cobalt ferrite/MXene nanoenzymes for drug-free phototherapy in bacterial infection treatment. RSC Adv 2022;12:11090–11099.
4. Ji SF, Jiang B, Hao HG, et al. Matching the kinetics of natural enzymes with a single-atom iron nanozyme. Nat Catal 2021;4:407–417.
5. Chen Y, Wang P, Hao H, et al. Thermal atomization of platinum nanoparticles into single atoms: An effective strategy for engineering high-performance nanozymes. J Am Chem Soc 2021;143:18643–18651.
6. Zhang L, Qin Z, Sun H, et al. Nanoenzyme engineered neutrophil-derived exosomes attenuate joint injury in advanced rheumatoid arthritis via regulating inflammatory environment. Bioact Mater 2022;18:1–14.
7. Liu ZH, Du Y, Zhang P, Zhuang Z, Wang D. Bringing catalytic order out of chaos with nitrogen-doped ordered mesoporous carbon. Matter 2021;4:3161–3194.
8. Cheng G, Chen J, Wang Q, et al. Promoting osteogenic differentiation in pre-osteoblasts and reducing tibial fracture healing time using functional nanofibers. Nano Res 2018;11:3658–3677.
9. Fahmy MA, Abdelaal AA, Hassan SI, et al. Antiparasitic and immunomodulating effects of nitazoxanide, ivermectin and selenium on Cryptosporidium infection in diabetic mice. Rev Bras Parasitol Vet 2021;30:e012121.
10. Goel V, Jain A, Sharma G, et al. Evaluating the efficacy of nitazoxanide in uncomplicated amebic liver abscess. Indian J Gastroenterol 2021;40:272–280.
11. Rossignol JF. Nitazoxanide: A first-in-class broad-spectrum antiviral agent. Antiviral Res 2014;110:94–103.
12. Wang YM, Lu JW, Lin CC, et al. Antiviral activities of niclosamide and nitazoxanide against chikungunya virus entry and transmission. Antiviral Res 2016;135:81–90.
13. Irabuena C, Scarone L, de Souza GE, et al. Synthesis and antiplasmodial assessment of nitazoxanide and analogs as new antimalarial candidates. Med Chem Res 2022;31:426–435.
14. Hickson SE, Margineantu D, Hockenbery DM, Simon JA, Geballe AP. Inhibition of vaccinia virus replication by nitazoxanide. Virology 2018;518:398–405.
15. Riccio A, Santopolo S, Rossi A, Piacentini S, Rossignol JF, Santoro MG. Impairment of SARS-CoV-2 spike glycoprotein maturation and fusion activity by nitazoxanide: An effect independent of spike variants emergence. Cell Mol Life Sci 2022;79:227.
16. Cadegiani FA, Goren A, Wambier CG, McCoy J. Early COVID-19 therapy with azithromycin plus nitazoxanide, ivermectin or hydroxychloroquine in outpatient settings significantly improved COVID-19 outcomes compared to known outcomes in untreated patients. New Microbes New Infect 2021;43:100915.
17. Martins-Filho PR, Barreto-Alves JA, Fakhouri R. Potential role for nitazoxanide in treating SARS-CoV-2 infection. Am J Physiol Lung Cell Mol Physiol 2020;319:L35–L36.
18. Mitchell J, Lo KWH. Small molecule-mediated regenerative engineering for craniofacial and dentoalveolar bone. Front Bioeng Biotechnol 2022;10:1003936.
19. Jin C, Zhang P, Zhang M, et al. Inhibition of SLC7A11 by sulfasalazine enhances osteogenic differentiation of mesenchymal stem cells by modulating BMP2/4 expression and suppresses bone loss in ovariectomized mice. J Bone Miner Res 2017;32:508–521.
20. He JY, Cheng M, Ye JL, et al. YY1-induced lncRNA XIST inhibits cartilage differentiation of BMSCs by binding with TAF15 to stabilizing FUT1 expression. Regen Ther 2022;20:41–50.
21. Rehman FU, Zhao C, Wu C, et al. Synergy and translation of allogenic bone marrow stem cells after photodynamic treatment of rheumatoid arthritis with tetra sulfonatophenyl porphyrin and TiO2 nanowhiskers. Nano Res 2016;9:3305–3321.
22. Yu M, Lei B, Gao CB, et al. Optimizing surface-engineered ultra-small gold nanoparticles for highly efficient miRNA delivery to enhance osteogenic differentiation of bone mesenchymal stromal cells. Nano Res 2017;10:49–63.
23. Xu C, Xiao L, Cao YX, et al. Mesoporous silica rods with cone shaped pores modulate inflammation and deliver BMP-2 for bone regeneration. Nano Res 2020;13:2323–2331.
24. Kumar N, Saraber P, Ding Z, Kusumbe AP. Diversity of vascular niches in bones and joints during homeostasis, ageing, and diseases. Front Immunol 2021;12:798211.
25. Zhang H, Xu R, Li B, et al. LncRNA NEAT1 controls the lineage fates of BMSCs during skeletal aging by impairing mitochondrial function and pluripotency maintenance. Cell Death Differ 2022;29:351–365.
26. Yue R, Zhou BO, Shimada IS, Zhao Z, Morrison SJ. Leptin receptor promotes adipogenesis and reduces osteogenesis by regulating mesenchymal stromal cells in adult bone marrow. Cell Stem Cell 2016;18:782–796.
27. Wang ZX, Luo ZW, Li FX, et al. Aged bone matrix-derived extracellular vesicles as a messenger for calcification paradox. Nat Commun 2022;13:1453.
28. Lu L, Tang M, Li J, et al. Gut microbiota and serum metabolic signatures of high-fat-induced bone loss in mice. Front Cell Infect Microbiol 2021;11:788576.
29. Yu LB, Xie MX, Zhang FJ, Wan C, Yao X. TM9SF4 is a novel regulator in lineage commitment of bone marrow mesenchymal stem cells to either osteoblasts or adipocytes. Stem Cell Res Ther 2021;12:573.
30. Karadeniz F, Oh JH, Jo HJ, Seo Y, Kong CS. Myricetin 3-O-β-D-galactopyranoside exhibits potential anti-osteoporotic properties in human bone marrow-derived mesenchymal stromal cells via stimulation of osteoblastogenesis and suppression of adipogenesis. Cells 2021;10:2690.
31. Zhang YL, Liu L, Su YW, Xian CJ. miR-542-3p attenuates bone loss and marrow adiposity following methotrexate treatment by targeting sFRP-1 and Smurf2. Int J Mol Sci 2021;22:10988.
32. Kim SP, Da H, Wang L, Taketo MM, Wan M, Riddle RC. Bone-derived sclerostin and Wnt/β-catenin signaling regulate PDGFRα+ adipoprogenitor cell differentiation. FASEB J 2021;35:e21957.
33. Tang CY, Chen W, Luo Y, et al. Runx1 up-regulates chondrocyte to osteoblast lineage commitment and promotes bone formation by enhancing both chondrogenesis and osteogenesis. Biochem J 2020;477:2421–2438.
34. Law SM, Zheng JJ. Premise and peril of Wnt signaling activation through GSK-3β inhibition. iScience 2022;25:104159.

35. Zhu Y, Wang YM, Jia YC, Xu J, Chai Y. Catalpol promotes the osteogenic differentiation of bone marrow mesenchymal stem cells via the Wnt/β-catenin pathway. Stem Cell Res Ther 2019;10:37.
36. Wang R, Gao D, Zhou Y, et al. High glucose impaired estrogen receptor alpha signaling via β-catenin in osteoblastic MC3T3-E1. J Steroid Biochem Mol Biol 2017;174:276–283.
37. Rakedzon S, Neuberger A, Domb AJ, Petersiel N, Schwartz E. From hydroxychloroquine to ivermectin: What are the antiviral properties of anti-parasitic drugs to combat SARS-CoV-2? J Travel Med 2021;28:taab005.
38. Custodio H. Protozoan parasites. Pediatr Rev 2016;37:59–71.
39. Shakya A, Bhat HR, Ghosh SK. Update on nitazoxanide: A multifunctional chemotherapeutic agent. Curr Drug Discov Technol 2018;15:201–213.
40. Walsh KF, McAulay K, Lee MH, et al. Early bactericidal activity trial of nitazoxanide for pulmonary tuberculosis. Antimicrob Agents Chemother 2020;64:e01956-19.
41. Kiehl IGA, Riccetto E, Salustiano ACC, et al. Boosting bladder cancer treatment by intravesical nitazoxanide and bacillus calmette-guérin association. World J Urol 2021;39:1187–1194.
42. Senkowski W, Zhang X, Olofsson MH, et al. Three-dimensional cell culture-based screening identifies the anthelmintic drug nitazoxanide as a candidate for treatment of colorectal cancer. Mol Cancer Ther 2015;14:1504–1516.
43. Jin H, Ji Y, Cui Y, Xu L, Liu H, Wang J. Simvastatin-incorporated drug delivery systems for bone regeneration. ACS Biomater Sci Eng 2021;7:2177–2191.
44. Yu Y, Oh SY, Kim HY, Choi JY, Jo SA, Jo I. Valproic acid-induced CCN1 promotes osteogenic differentiation by increasing CCN1 protein stability through HDAC1 inhibition in tonsil-derived mesenchymal stem cells. Cells 2022;11:534.
45. Dong K, Zhou WJ, Liu ZH. Metformin enhances the osteogenic activity of rat bone marrow mesenchymal stem cells by inhibiting oxidative stress induced by diabetes mellitus: An in vitro and in vivo study. J Periodontal Implant Sci 2023;53:54–68.
46. Lü Z, Li X, Li K, et al. Structure-activity study of nitazoxanide derivatives as novel STAT3 pathway inhibitors. ACS Med Chem Lett 2021;12:696–703.
47. Ye C, Wei M, Huang H, et al. Nitazoxanide inhibits osteosarcoma cells growth and metastasis by suppressing AKT/mTOR and Wnt/β-catenin signaling pathways. Biol Chem 2022;403:929–943.
48. Khan SA, Lee TKW. Investigations of nitazoxanide molecular targets and pathways for the treatment of hepatocellular carcinoma using network pharmacology and molecular docking. Front Pharmacol 2022;13:968148.